GaAsSb-capped InAs quantum dots: From enlarged quantum dot height to alloy fluctuations

J. M. Ulloa,[1,*] R. Gargallo-Caballero,[1] M. Bozkurt,[2] M. del Moral,[1] A. Guzmán,[1] P. M. Koenraad,[2] and A. Hierro[1]
[1]*Institute for Systems based on Optoelectronics and Microtechnology (ISOM), Universidad Politecnica de Madrid, Ciudad Universitaria s/n, 28040 Madrid, Spain*
[2]*Photonics and Semiconductor Nanophysics, Department of Applied Physics, Eindhoven University of Technology, P.O. Box 513, NL-5600 MB Eindhoven, The Netherlands*
(Received 24 November 2009; revised manuscript received 17 February 2010; published 6 April 2010)

The Sb-induced changes in the optical properties of GaAsSb-capped InAs/GaAs quantum dots (QDs) are shown to be strongly correlated with structural changes. The observed redshift of the photoluminescence emission is shown to follow two different regimes. In the first regime, with Sb concentrations up to ~12%, the emission wavelength shifts up to ~1280 nm with a large enhancement of the luminescence characteristics. A structural analysis at the atomic scale by cross-sectional scanning tunneling microscopy shows that this enhancement arises from a gradual increase in QD height, which improves carrier confinement and reduces the sensitivity of the excitonic band gap to QD size fluctuations within the ensemble. The increased QD height results from the progressive suppression of QD decomposition during the capping process due to the presence of Sb atoms on the growth surface. In the second regime, with Sb concentrations above ~12%, the emission wavelength shifts up to ~1500 nm, but the luminescence characteristics progressively degrade with the Sb content. This degradation at high Sb contents occurs as a result of composition modulation in the capping layer and strain-induced Sb migration to the top of the QDs, together with a transition to a type-II band alignment.

DOI: 10.1103/PhysRevB.81.165305 PACS number(s): 78.67.Hc, 78.55.Cr, 81.15.Hi, 68.37.Ef

I. INTRODUCTION

Quantum dots (QDs) based on semiconductor materials have a great potential for applications in optoelectronic devices. In particular, much effort has been dedicated in the past few years to develop QD laser diodes emitting at the telecommunication bands. One recent approach is based on the possibility of extending the emission wavelength of self-assembled InAs/GaAs QDs to the 1.3 and 1.55 μm regions by using a GaAsSb capping layer.[1–5] Room-temperature photoluminescence (PL) at 1.6 μm has already been reported from these structures.[3,4] The strong observed redshift has been typically attributed to a type-II band alignment for high Sb contents, with the hole wave function being localized out of the QD in the GaAsSb capping layer.[3,4,6–9] Nevertheless, apart from a few studies dedicated to analyze the emission from type-II samples,[6–10] not much attention has been paid to the evolution of the optical properties of GaAsSb-capped InAs/GaAs QDs with the amount of Sb in the capping layer. Moreover, the effect that different Sb contents could have in the structural properties of the QDs is still unknown. The fact that GaAsSb acts as a strain reducing layer for InAs/GaAs QDs, together with the surfactant effect of Sb, could lead to an altered capping process that could modify the final size and/or shape of the QDs. It is well known that strong QD size and shape changes usually take place during the capping process and that these changes are dependent on the capping material used.[11–17] Indeed, a size modification compared to GaAs-capped QDs has already been observed in GaAsSb-capped QDs with 22% Sb,[18] but the effect of small amounts of Sb remains unknown and a dependence on the Sb content has never been established. These structural changes are of crucial relevance because they will strongly affect the optical properties of the QD system. Therefore, detailed information about the QD-capping layer structure as a function of the Sb content and its relationship with the optical properties would be very useful in order to understand the physics of GaAsSb-capped QDs and to fully exploit these structures for telecommunication wavelength applications.

In this work, we have used PL, cross-sectional scanning tunneling microscopy (X-STM) and atomic force microscopy (AFM) to correlate the Sb-induced changes in the optical properties of the QDs with structural changes at the atomic scale, revealing that only the Sb-induced structural changes can explain the two different optical regimes that we find when the Sb content in the capping layer is gradually increased. We show that within the first regime the QD height can be controllably tuned allowing to obtain room-temperature PL emission at 1.3 μm with improved characteristics compared to the reference GaAs-capped QDs.

II. EXPERIMENTAL DETAILS

The samples were grown by solid source molecular beam epitaxy on n^+ Si-doped (100) GaAs substrates. A series of 11 samples containing a single QD layer was grown for PL studies. In all these samples, 2.7 monolayers (MLs) of InAs were deposited at 450 °C and 0.04 ML/s on an intrinsic GaAs buffer layer. After InAs deposition, a 30 s growth interruption under arsenic flux was performed during which the temperature was raised to 470 °C. The QDs were subsequently capped with a nominally 4.5-nm-thick $GaAs_{1-x}Sb_x$ layer grown at 470 °C followed by 10 MLs of GaAs grown at the same temperature. The Sb content was nominally changed from 0 to 25% by keeping a constant high arsenic flux and increasing the antimony flux resulting in values of the Sb_4/As_4 beam equivalent pressure ratio between 0 and 0.05. 200–250 nm of GaAs grown at 580 °C were finally deposited on top of the GaAsSb capping. A layer of similar uncapped QDs was also grown on the surface of every

sample for AFM measurements. Four of the GaAsSb-capped QD layers with different Sb contents were reproduced in a single sample (separated from each other by 50 nm of GaAs) for X-STM measurements. The surface of this sample was also covered with a layer of uncapped QDs grown under the same conditions as those from the underlying layers.

The PL was measured at room temperature using a He-Ne laser as the excitation source. The emitted light was dispersed through a 1 m spectrometer and detected with a liquid nitrogen cooled Ge detector. The X-STM measurements were performed on a (1 1 0) surface plane of *in situ* cleaved samples under UHV ($p < 4 \times 10^{-11}$ Torr) conditions at room temperature. Polycrystalline tungsten tips prepared by electrochemical etching were used. The images were obtained in constant current mode at high negative voltages (~3 V). Standard tapping mode AFM measurements with antimony-doped Si tips were used to characterize the surface QDs.

III. RESULTS AND DISCUSSION

A. Optical properties

As shown in Fig. 1(a), by gradually increasing the Sb content in the capping layer the emission wavelength of the QDs can be redshifted, reaching almost 1.5 μm. All the QDs in these samples are grown under the same conditions and have a similar size before capping (7.5 ± 0.5 nm height and 26 ± 2 nm base length), as measured by AFM in surface QDs. This means that the differences giving rise to the redshift originated during the capping process. The emission wavelength can therefore be controllably tuned within a very wide region (1150–1500 nm) by exclusively increasing the Sb content in the capping layer. However, two clear different optical regimes (regimes I and II) are observed as the Sb content is increased [Fig. 1(b)]. For low Sb contents, the PL emission is progressively improved [reduced full width at half maximum (FWHM) and increased integrated intensity], reaching its optimum at a peak wavelength of ~1280 nm. For higher wavelengths (higher Sb contents) the PL is gradually degraded with increasing Sb becoming very broad for the longest wavelengths. Indeed, the presence of the first regime allows to obtain PL emission at 1.3 μm with significantly improved optical properties compared to the shorter wavelength PL of the reference GaAs-capped InAs/GaAs QDs. A similar enhancement of the PL integrated intensity by one order of magnitude at 1.3 μm has been obtained by exposing the QDs to Sb during 10 s and capping them with 3 ML of GaAs followed by 2 ML of GaSb.[19] Nevertheless, the enhancement was attributed in that case to Sb incorporation inside the QDs,[19,20] while in our case the physical reasons are completely different, as it will be shown later.

Previous works have assigned the Sb-induced changes in the optical properties to the reduced strain and the transition from a type-I to a type-II band alignment (holes are confined in the capping layer).[1–10] However, the evolution of the PL spectra with the Sb content within these two optical regimes cannot be explained by only considering these mechanisms. From PL measurements as a function of excitation power we see that the transition from a type-I to a type-II alignment happens at a longer wavelength (~1350 nm) than the onset

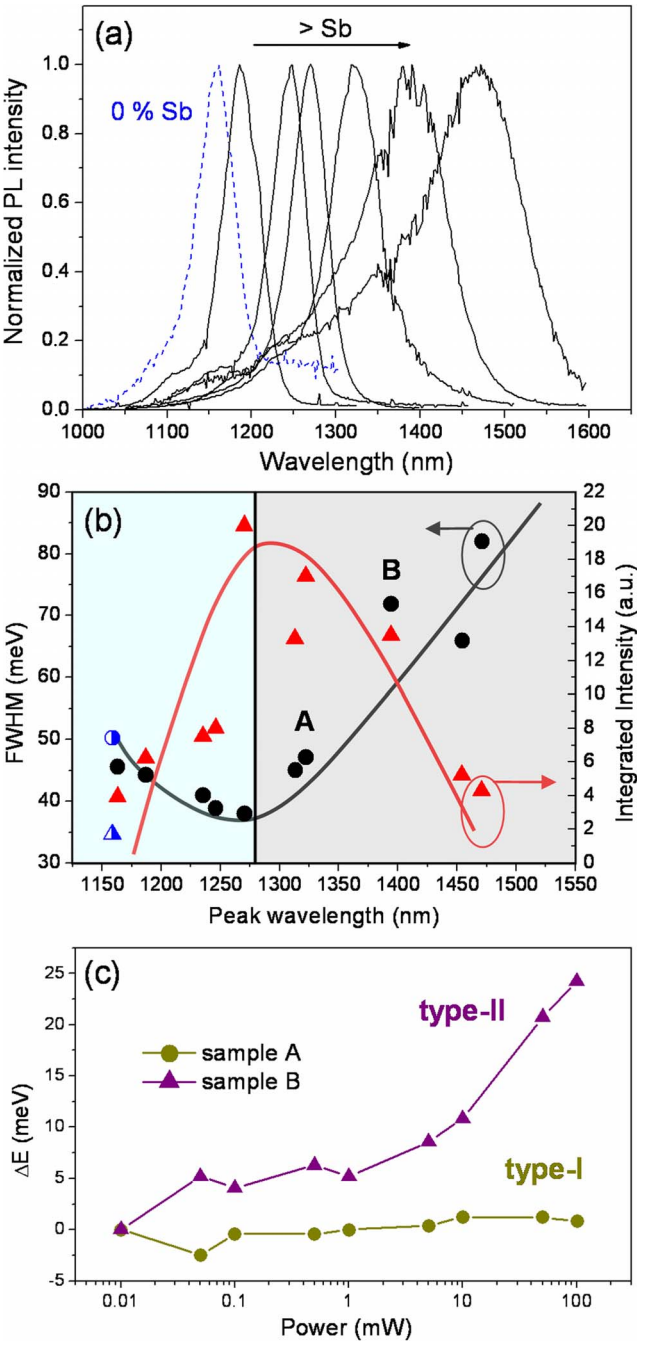

FIG. 1. (Color online) (a) Normalized room-temperature PL spectra from a selection of the QD layers with increasing amount of Sb in the capping layer. (b) Dependence of the FWHM and integrated PL intensity on the peak wavelength. The half-filled signs correspond to the 0% Sb case. Lines are guides for the eyes. The two different background colors indicate the two different optical regimes. (c) Relative blueshift of the PL peak energy with excitation power for the samples labeled as A and B in Fig. 1(b).

for the degradation of the optical properties (~1280 nm). Indeed, sample B is the first sample to show a clear type-II band alignment behavior that is also present in all the QD layers emitting at longer wavelengths. This is evident from the observed blueshift of the PL peak energy with excitation power in those samples, which is not present in the shorter

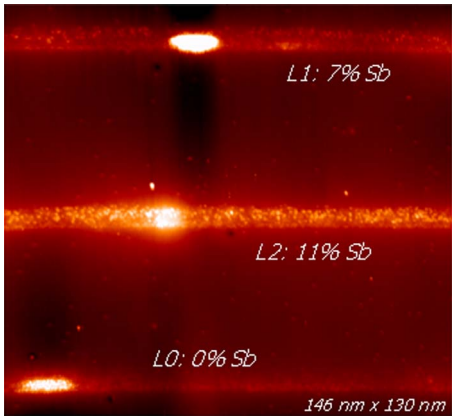

FIG. 2. (Color online) X-STM topography image ($V=-3$ V) of the first three layers of the sample designed for X-STM measurements. The GaAsSb layer with higher amount of Sb appears brighter in the image. The Sb contents shown are obtained from the analysis of the images. One QD in each layer can be observed.

wavelength layers, as shown in Fig. 1(c) for samples A and B. This blueshift arises from the band bending effect induced by the spatially separated photoexcited carriers in a type-II band alignment.[6] In the type-II samples, emission from excited states is present even at low excitation powers due to the increased carrier lifetime[7] [see the high energy tail in the PL spectra of the type-II samples in Fig. 1(a)]. In those cases, the FWHM used for comparison is that of the ground-state emission, and consequently, the presence of the excited states emission is not the reason for the strong FWHM broadening at long wavelengths. The observed evolution of the PL spectra must therefore be related also to structural changes.

B. Structural properties

A X-STM large scale topography image of the sample with four QD layers is shown in Fig. 2. The Sb content in the capping layer was different in each layer, starting from 0% (reference GaAs-capped QDs) in the first layer. Only three layers (from now on L0, L1, and L2) are visible in the image. The last layer, with the highest Sb content, could not be analyzed due to bad cleavage probably due to too much accumulated strain. Nevertheless, a layer with high Sb content grown in another sample could be measured successfully (from now on called L3). From these high voltage (−3 V) images, the Sb content in the capping layer can be deduced by analyzing the outward relaxation of the cleaved surface. Under high voltage conditions, the electronic contrast is strongly suppressed and the measurements reflect mainly the topographic contrast, which is due to the outward relaxation of the cleaved surface due to the compressive strain stemming from the QDs and the wetting layer (WL).[21,22] In our case, since the GaAsSb capping layer is also compressively strained, it will also contribute to the outward relaxation. The relaxation of the layer far from a QD (averaged over a ~80 nm wide region to avoid any possible effect of alloy fluctuations) was compared to calculations from continuum elasticity theory (Fig. 3). A finite element calculation was performed to solve the three-dimensional problem, in which an isotropic material is considered. Both the wetting layer and the capping layer were considered in the calculation and In and Sb segregations were also included. The measured thickness of the GaAsSb layer (4.0 ± 0.5 nm) is introduced in the model and the composition is changed until a good fit to the experimental profile is obtained. From the fits shown in Fig. 3, the Sb content is deduced to be 0%, 7%, 11%, and 22% for L0, L1, L2, and L3, respectively.

A high-resolution image of a QD in L0, L1, and L3 can be seen in Figs. 4(a)–4(c), respectively. The measurement conditions (negative voltage) allow imaging group V elements so that the bright spots in images (b) and (c) represent individual Sb atoms in the As matrix (due to the different size and bonding configuration, Sb atoms appear brighter than As atoms). The bright spots in image (a) represent individual In atoms, which are visible through their distortion of the surrounding As atoms. The GaAsSb layer appears clearly as a distinct layer, which is hardly intermixed with the QDs and the WL (see also Fig. 2). The interface between the QD and the capping layer is well defined especially in the lower Sb content layers L1 and L2 [see Fig. 4(b)]. This suggests that there is no Sb incorporation into the QDs. Further support for this conclusion can be obtained by applying a local mean equalization filter to the images (which eliminates the background contrast due to strain relaxation and enhances the contrast of individual Sb atoms). The average contrast between adjacent atoms in filtered images is the same in GaAsSb-capped QDs than in the QDs of the reference layer. It can therefore be concluded that there is no Sb inside the QDs contrary to what has been observed in InAs/GaAs QDs capped directly with 2.2 ML of GaSb.[20]

Significant differences between the QDs in the different layers are already clear from these images. The size and shape of the QDs in each layer can be deduced by a statistical analysis of the relationship between the height and the base length in a large number of QDs. Considering the high uniformity observed by AFM [see Fig. 6(a)], it is assumed for the analysis that all the dots in each layer are identical. After analyzing ~15 QDs in each layer, a linear dispersion, similar to that obtained in Ref. 23, is found, indicating that the QDs have an ellipsoidal or lens shape (as also apparent from Fig. 4) with a base diameter of 24 ± 1 nm. This correlates very well with the 26 ± 2 nm diameter measured by AFM in similar surface QDs.

However, the capped QD height increases with the Sb content, as shown in Fig. 5, in which the QD height normalized to the height of surface uncapped QDs is plotted as a function of the Sb content in the capping layer. The height differences must be originated during the capping process: the strong QD decomposition that takes place during capping with GaAs (Refs. 11–17) is reduced by the presence of Sb. Moreover, the reduction is proportional to the amount of Sb in the capping layer. The result is that the QD height is progressively increased when the amount of Sb in the capping layer increases. The dissolution process is found to be completely suppressed for an Sb content of 22% (the QD height measured by X-STM is the same that the one measured by AFM in uncapped QDs) but the linear regression in the figure shows that QD dissolution stops completely for a smaller Sb content of ~14%. For higher Sb contents, no

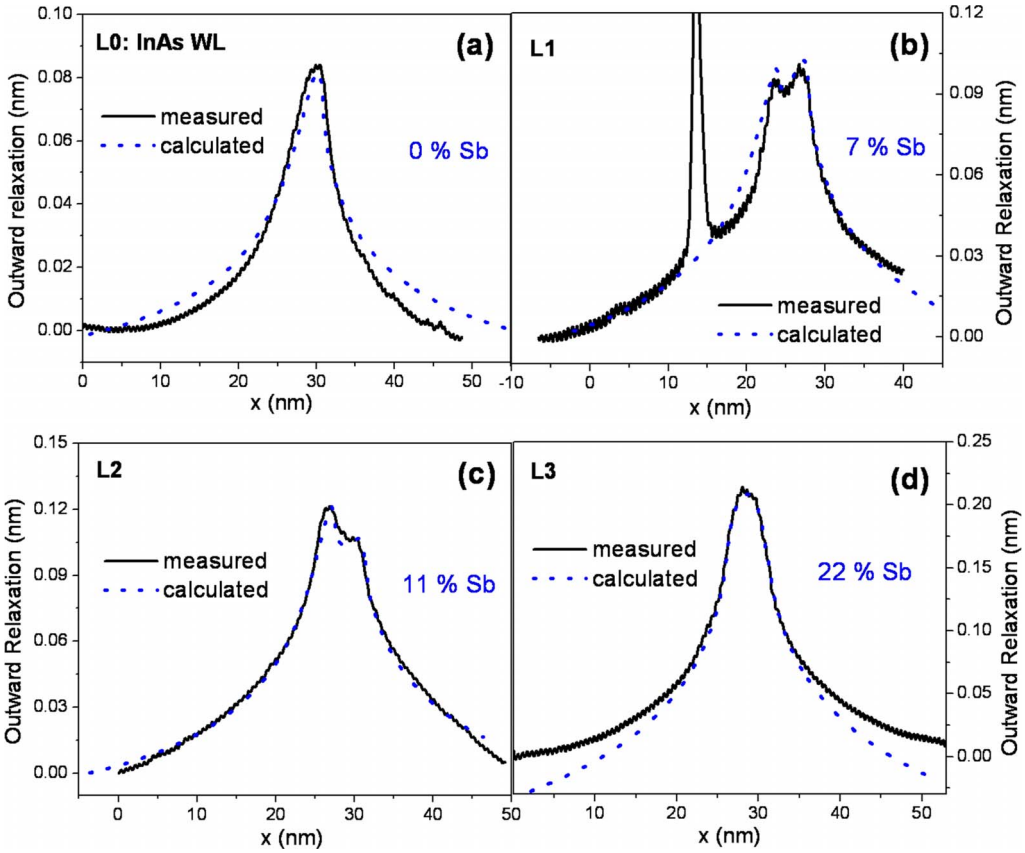

FIG. 3. (Color online) Measured (solid line) and calculated (dotted line) outward relaxation profiles of the four different layers studied by X-STM. The amount of Sb deduced was 0%, 7%, 11%, and 22% [(a), (b), (c), and (d), respectively]. The measured profiles are averaged to a wide region of ~80 nm to avoid any possible effect of alloy fluctuations. The spike observed in Fig. 3(b) is due to a measurement artifact. The origin of this artifact is an adsorbate on the cleaved surface which is pushed by the tip in the direction along the WL.

further change in the QD height is expected. It is possible, therefore, to controllably tune the height of the InAs QDs by changing the Sb content in the capping layer between 0 and ~14%.

C. Regime I: from 1150 to 1280 nm

As we just showed, the QD height progressively increases with the Sb content and can be more than doubled by adding 14% Sb (the base length is found to be unaffected by the amount of Sb). This should strongly affect the optical properties, not only by redshifting the wavelength but also by increasing the PL intensity due to stronger carrier confinement.[24] The resulting enhancement of the electron-hole wave function overlap is likely the reason for the improved PL integrated intensity obtained when the Sb content is initially increased. Moreover, since the dependence of the energy of the confined levels on QD size decreases when the QD size increases,[25,26] taller QDs will show less dispersion in the effective band-gap energy for the same size fluctuations within the ensemble. This could explain the observed initial narrowing of the PL with the Sb content [Fig. 1(b)]. The RT PL peak wavelength of L2 (11% Sb) is 1268 nm, very close to the ~1280 nm peak wavelength of the optimum PL spectrum. This means that regime I takes place for Sb contents up to ~11–12% coinciding with the region of progressively increased QD height (up to ~14% Sb). Therefore, the region of improved PL characteristics can be directly correlated with an increased QD height.

The presence of Sb in the growth front must have the effect of reducing the In-Ga intermixing, the main reason for QD decomposition during capping,[11,12,17] and this reduction is proportional to the amount of Sb within regime I. This phenomenon is likely due to the surfactant effect of Sb, which reduces the adatom surface diffusion on the growth front. Since intermixing takes place from the very initial stages of the capping process,[11,16,17] we can further confirm the X-STM results by an AFM analysis of surface QDs in which only 3 ML of GaAs(Sb) are deposited. Once the thin capping layer is deposited, the sample is kept for 30 s under As_4 and then it is quickly cooled down. Figure 6 shows AFM images of uncapped QDs [Fig. 6(a)] and the same QDs capped with 3 ML of GaAs [Fig. 6(b)] or 3 ML of GaAsSb [Fig. 6(c)]. When capping with GaAs, a strong intermixing occurs and the QDs are strongly dissolved resulting in an InGaAs thin layer.[17] This is why they are not visible in the image (only the few very big QDs initially present are still visible). The situation is very different when capping with GaAsSb. The QDs are still visible indicating a strong reduction in In-Ga intermixing and In segregation out of the QDs. Moreover, if the amount of Sb in the 3 ML of GaAsSb is increased, the height of the QDs increases [see Fig. 6(d)]

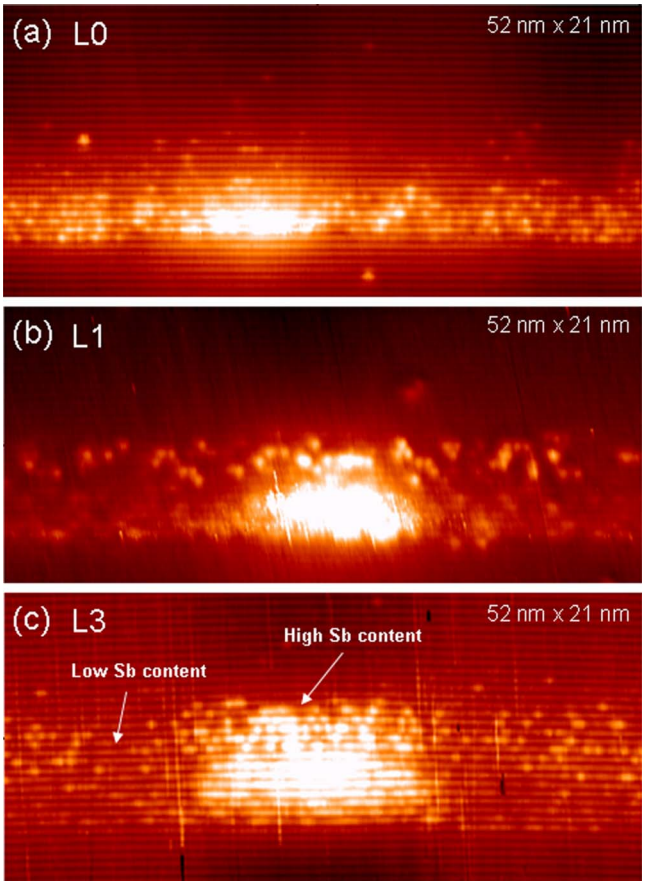

FIG. 4. (Color online) Filled states topography images of a QD in (a) L0, (b) L1, and (c) L3. In image (a) the bright spots correspond to In atoms. In images (b) and (c) the bright spots correspond to Sb atoms in the As matrix.

confirming the correlation between the amount of Sb and the degree of reduced decomposition during capping (or the degree of increased QD height). During the decomposition process, the In which leaves the QDs moves back to the WL.

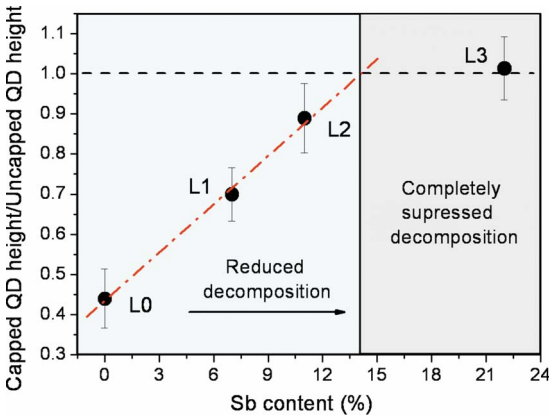

FIG. 5. (Color online) QD height normalized to the height of the equivalent uncapped QDs as a function of the Sb content in the four different layers studied by X-STM. A value of 1.0 indicates a completely suppressed decomposition process. The red dash-dotted line is a linear fit to the values of L0, L1, and L2. The two different background colors indicate the two different regimes.

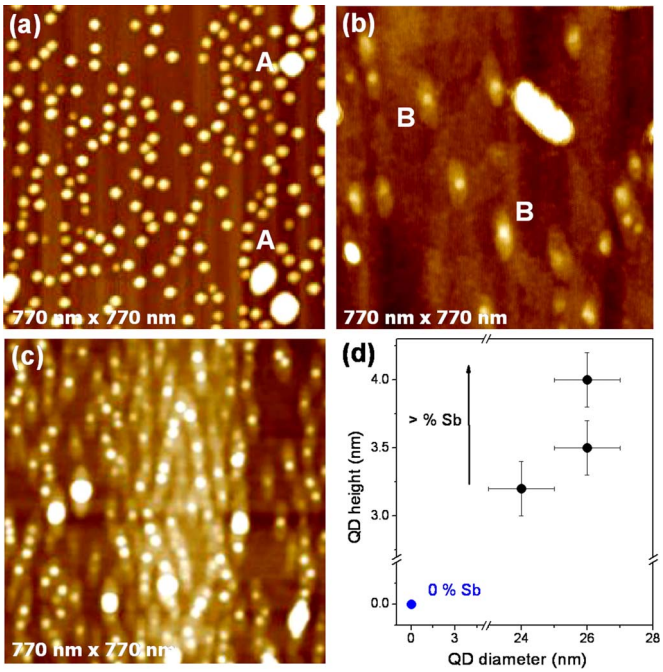

FIG. 6. (Color online) AFM images of (a) uncapped QDs, (b) QDs capped with 3 ML GaAs, and (c) QDs capped with 3 ML GaAsSb. The z range is 20 nm in (a), and 10 nm in (b) and (c). Image (d) shows the QD height and base length measured by AFM in QDs with different amounts of Sb in the 3 ML capping.

This is evident from the fact that the amount of InAs in the WL is progressively reduced when the Sb content increases: from the fits shown in Fig. 3, the amount of InAs in the WL of L0 (0% Sb), L1 (7% Sb), and L2 (11% Sb) is found to be 1.50, 1.32, and 1.16 MLs, respectively (the fact that the outward relaxation peaks of the WL and capping layer are distinguishable eliminates any uncertainty about the Sb and In contents deduced). Therefore, there is a strong mass transport process during capping with GaAs, but the In atoms from the top of the QDs are not being relocated on the QD base,[27] they contribute to form a thicker WL.

D. Regime II: from 1280 to 1500 nm

The previous results can explain the initial improvement in the PL spectra, but not the subsequent degradation. A second mechanism, competing with the first one, is likely responsible for this second optical regime. This mechanism is found to be related to alloy fluctuations in the capping layer. Figure 7 shows filled states high voltage images of L1 [Fig. 7(a)] and L3 [Fig. 7(b)]. While in L1 there is no significant difference in brightness along the layer, in L3 some clearly brighter regions appear. As explained before, in high voltage images the relaxation is proportional to the strain and, therefore, to the Sb content: the brighter regions are Sb-rich regions and the darker ones Sb-poor regions. The Sb distribution is quite homogeneous in low Sb content samples, but for high Sb contents, Sb-rich clusters with a lateral size between 10 and 20 nm appear in the capping layer [see the arrows in Fig. 7(b)]. This strong composition modulation could be due to the large miscibility gap of GaAsSb.[28] By comparing the

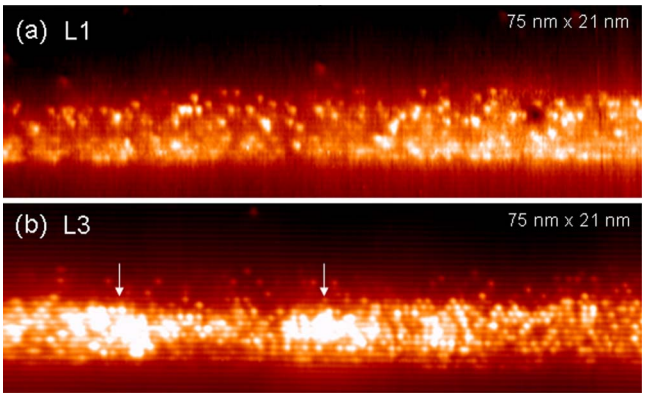

FIG. 7. (Color online) Filled states topography images of the WL and capping layer of (a) L1 and (b) L3. A clear contrast inhomogeneity is present in L3 in which Sb-rich clusters (indicated by the arrows) are formed.

outward relaxation profile between Sb-rich and Sb-poor regions, the absolute value of the Sb fluctuations can be estimated to be 2%, 4%, and 12% in L1, L2, and L3, respectively. The alloy fluctuations are very small for low Sb contents but they increase with Sb, becoming very strong for Sb contents of 22%.

The observed clusters can act as GaAsSb/GaAs QDs, trapping holes and reducing the carrier injection efficiency in the InAs QDs, which would reduce the PL integrated intensity. Moreover, the composition modulation can be enhanced by the strain field of the QDs which propagates into the matrix. Since GaSb has a very similar lattice constant to InAs, from the point of view of the strain it will be favorable for Sb to accumulate on top of the partially relaxed InAs QDs (a similar process has been observed for InGaAs capping and columnar QD growth).[14,29,30] This is clearly observed in the X-STM measurements of L3, in which the amount of Sb on top of the QDs is much higher than around them [see Fig. 4(c)]. In the low Sb content samples, in which alloy fluctuations are very small, there is no Sb accumulation on top of the QDs [see Fig. 4(b)]. In this case, all of the QDs are covered by a very similar and uniform layer and therefore they have the same strain state and band offsets. The result is that the PL of the ensemble is narrow. When the Sb content is increased, the composition modulation becomes significant, introducing inhomogeneities in the composition of the capping layer on top of a single QD and between different QDs, which results in a PL broadening. The PL broadening is enhanced for the high Sb content type-II samples. In this case, the hole wave function is confined in the capping layer on top of the QDs and, therefore, different Sb contents on top of the QDs will have a much stronger impact on the hole energy levels. This is likely the reason for the strong increase in the FWHM of the type-II samples compared to the type-I ones. The observed PL degradation in regime II can therefore be explained by the presence of alloy fluctuations in the capping layer and strain-induced Sb accumulation on top of the QDs, together with the transition to a type-II band alignment.

We suggest that the Sb accumulation locally above the QDs is a step toward their extension by an Sb rich top. The interface between the QDs and the Sb-rich capping is starting to be less defined in the highest Sb content sample [see Fig. 4(c)], which means that a weak intermixing (affecting only the first monolayer on top of the QD) could be already starting for an Sb content of 22%.

It must be noticed that, despite the presence of alloy fluctuations and the type-II band alignment, the integrated intensity of the longest wavelength samples is still slightly larger than that of the reference sample, indicating that these samples could still be very useful for applications in which a broad spectral range luminescence can be an advantage, like in semiconductor optical amplifiers.[31] The fact that the PL integrated intensity is not drastically decreased as a result of the transition to a type-II band alignment is likely due to the Sb accumulation on top of the QDs, which localizes the holes very close to the QDs and increases the electron-hole wave function overlap in comparison to a standard type-II QD system.

IV. CONCLUSIONS

While increasing the Sb content in GaAsSb-capped InAs/GaAs QDs allows to shift the emission to longer wavelengths, two different optical regimes are clearly observed, which can only be explained by taking into account the structural changes. For small Sb contents up to ~12–14%, the QD height increases progressively with the amount of Sb, which improves the PL properties through an improved carrier confinement and a reduced sensitivity of the confined energy levels to size fluctuations. On the other hand, composition modulation in the capping layer also increases with the amount of Sb, and influences the PL emission for high Sb contents above ~12%, making the spectra broader and less intense. For high Sb contents of ~22%, the composition modulation is enhanced by the strain field of the QDs giving rise to inhomogeneous Sb accumulation on top of the QDs. Since this happens mainly in the type-II structures, with the holes confined in the capping layer on top of the QDs, it strongly affects the hole energy levels, resulting in a very broad PL emission.

ACKNOWLEDGMENTS

This work was supported by the Comunidad de Madrid through the project NANOCOMIC (Grant No. S05051ESP-0200), by the European Union through the SANDiE Network of Excellence (Contract No. NMP4-CT-2004-500101), and by STW-VICI Grant No. 6631. J.M.U. would like to thank A. G. Taboada and J. M. Ripalda from Instituto de Microelectrónica de Madrid, CNM (CSIC), Spain for helpful discussions.

*jmulloa@die.upm.es

[1] K. Akahane, N. Yamamoto, and N. Ohtani, Physica E (Amsterdam) **21**, 295 (2004).

[2] H. Y. Liu, M. J. Steer, T. J. Badcock, D. J. Mowbray, M. S. Skolnick, P. Navaretti, K. M. Groom, M. Hopkinson, and R. A. Hogg, Appl. Phys. Lett. **86**, 143108 (2005).

[3] J. M. Ripalda, D. Granados, Y. González, A. M. Sánchez, S. I. Molina, and J. M. García, Appl. Phys. Lett. **87**, 202108 (2005).

[4] H. Y. Liu, M. J. Steer, T. J. Badcock, D. J. Mowbray, M. S. Skolnick, F. Suarez, J. S. Ng, M. Hopkinson, and J. P. R. David, J. Appl. Phys. **99**, 046104 (2006).

[5] T. Matsuura, T. Miyamoto, M. Ohta, and F. Koyama, Phys. Status Solidi C **3**, 516 (2006).

[6] T. T. Chen, C. L. Cheng, Y. F. Chen, F. Y. Chang, H. H. Lin, C.-T. Wu, and C.-H. Chen, Phys. Rev. B **75**, 033310 (2007).

[7] Y. D. Jang, T. J. Badcock, D. J. Mowbray, M. S. Skolnick, J. Park, D. Lee, H. Y. Liu, M. J. Steer, and M. Hopkinson, Appl. Phys. Lett. **92**, 251905 (2008).

[8] W.-H. Chang, Y.-A. Liao, W.-T. Hsu, M.-C. Lee, P.-C. Chiu, and J.-I. Chyi, Appl. Phys. Lett. **93**, 033107 (2008).

[9] Y.-A. Liao, W.-T. Hsu, P.-C. Chiu, J.-I. Chyi, and W.-H. Chang, Appl. Phys. Lett. **94**, 053101 (2009).

[10] C. Y. Jin, H. Y. Liu, S. Y. Zhang, Q. Jiang, S. L. Liew, M. Hopkinson, T. J. Badcock, E. Nabavi, and D. J. Mowbray, Appl. Phys. Lett. **91**, 021102 (2007).

[11] J. M. Garcia, G. Medeiros-Ribeiro, K. Schmidt, T. Ngo, J. L. Feng, A. Lorke, J. Kotthaus, and P. M. Petroff, Appl. Phys. Lett. **71**, 2014 (1997).

[12] P. D. Siverns, S. Malik, G. McPherson, D. Childs, C. Roberts, R. Murray, B. A. Joyce, and H. Davock, Phys. Rev. B **58**, R10127 (1998).

[13] G. D. Lian, J. Yuan, L. M. Brown, G. H. Kim, and D. A. Ritchie, Appl. Phys. Lett. **73**, 49 (1998).

[14] J. M. Ulloa, C. Çelebi, P. M. Koenraad, A. Simon, E. Gapihan, A. Letoublon, N. Bertru, J. Drouzas, D. J. Mowbray, M. J. Steer, and M. Hopkinson, J. Appl. Phys. **101**, 081707 (2007).

[15] R. Leon, J. Wellman, X. Z. Liao, J. Zou, and D. J. H. Cockayne, Appl. Phys. Lett. **76**, 1558 (2000).

[16] P. B. Joyce, T. J. Krzyzewski, P. H. Steans, G. R. Bell, J. H. Neave, and T. S. Jones, Surf. Sci. **492**, 345 (2001).

[17] Q. Gong, P. Offermans, R. Nötzel, P. M. Koenraad, and J. H. Wolter, Appl. Phys. Lett. **85**, 5697 (2004).

[18] J. M. Ulloa, I. W. D. Drouzas, P. M. Koenraad, D. J. Mowbray, M. J. Steer, H. Y. Liu, and M. Hopkinson, Appl. Phys. Lett. **90**, 213105 (2007).

[19] J. M. Ripalda, D. Alonso-Álvarez, B. Alén, A. G. Taboada, J. M. García, Y. González, and L. González, Appl. Phys. Lett. **91**, 012111 (2007).

[20] S. I. Molina, A. M. Sánchez, A. M. Beltrán, D. L. Sales, T. Ben, M. F. Chisholm, M. Varela, S. J. Pennycook, P. L. Galindo, A. J. Papworth, P. J. Goodhew, and J. M. Ripalda, Appl. Phys. Lett. **91**, 263105 (2007).

[21] R. M. Feenstra, Physica B **273-274**, 796 (1999).

[22] D. M. Bruls, J. W. A. M. Vugs, P. M. Koenraad, H. W. M. Salemink, J. H. Wolter, M. Hopkinson, M. S. Skolnick, F. Long, and S. P. A. Gill, Appl. Phys. Lett. **81**, 1708 (2002).

[23] J. H. Blokland, M. Bozkurt, J. M. Ulloa, D. Reuter, A. D. Wieck, P. M. Koenraad, P. C. M. Christianen, and J. C. Maan, Appl. Phys. Lett. **94**, 023107 (2009).

[24] J. Johansen, S. Stobbe, I. S. Nikolaev, T. Lund-Hansen, P. T. Kristensen, J. M. Hvam, W. L. Vos, and P. Lodahl, Phys. Rev. B **77**, 073303 (2008).

[25] L.-W. Wang and A. Zunger, Phys. Rev. B **53**, 9579 (1996).

[26] H. Fu and A. Zunger, Phys. Rev. B **56**, 1496 (1997).

[27] G. Costantini, A. Rastelli, C. Manzano, P. Acosta-Diaz, R. Songmuang, G. Katsaros, O. G. Schmidt, and K. Kern, Phys. Rev. Lett. **96**, 226106 (2006).

[28] H. Mani, A. Joullie, F. Karouta, and C. Schiller, J. Appl. Phys. **59**, 2728 (1986).

[29] M. V. Maximov, A. F. Tsatsul'nikov, B. V. Volovik, D. S. Sizov, Yu. M. Shernyakov, I. N. Kaiander, A. E. Zhukov, A. R. Kovsh, S. S. Mikhrin, V. M. Ustinov, Zh. I. Alferov, R. Heitz, V. A. Shchukin, N. N. Ledentsov, D. Bimberg, Yu. G. Musikhin, and W. Neumann, Phys. Rev. B **62**, 16671 (2000).

[30] J. He, R. Nötzel, P. Offermans, P. M. Koenraad, Q. Gong, G. J. Hamhuis, T. J. Eijkemans, and J. H. Wolter, Appl. Phys. Lett. **85**, 2771 (2004).

[31] Z. Bakonyi, H. Su, G. Onishchukov, L. F. Lester, A. L. Gray, T. C. Newell, and A. Tünnermann, IEEE J. Quantum Electron. **39**, 1409 (2003).